EurJIC
European Journal of Inorganic Chemistry

Research Article
doi.org/10.1002/ejic.202200109

Chemistry Europe
European Chemical Societies Publishing

www.eurjic.org

Methoxido-Bridged Lacunary Heterocubane Oxidovanadium(IV) Cluster with Azo Ligands: Synthesis, X-ray Structure, Magnetic Properties, and Antiproliferative Activity

Satabdi Roy,[a, b] Michael Böhme,[c] Sudhir Lima,[a, c] Monalisa Mohanty,[a] Atanu Banerjee,[a] Axel Buchholz,[c] Winfried Plass,*[c] Sharan Rathnam,[d] Indranil Banerjee,[d, e] Werner Kaminsky,[f] and Rupam Dinda*[a]

Dedicated to Prof. Dr. Wolfgang Beck on the occasion of his 90th Birthday.

The new μ_3-methoxido bridged trinuclear vanadium(IV) complexes $[V^{IV}_3O_3(\mu_3\text{-OMe})(\mu_2\text{-OMe})_3(L^{1,2})_2]$ (**1** and **2**) have been synthesized using the azo ligands 1-(2-(thiazol-2-yl)diazenyl)naphthalene-2-ol (HL^1) and 2-(2-(thiazol-2-yl)diazenyl)-4-methylphenol (HL^2). X-ray crystallography revealed a trinuclear structure with a lacunary heterocubane $\{(VO)_3(\mu_3\text{-OMe})(\mu_2\text{-OMe})_3\}^{2+}$ core unit for complex **1**, which contains a central μ_3-methoxido bridge. All three vanadium centers are in a slightly distorted octahedral coordination environment. Magnetic and theoretical studies reveal an antiferromagnetic coupling between the three vanadium(IV) centers within the triangular arrangement in **1**. The complexes were also screened for *in vitro* cytotoxicity study against HeLa and HT-29 cancer cell lines. The results indicated that both the complexes are cytotoxic but possess varying specificity towards different cell types.

Introduction

The coordination chemistry of vanadium is attaining continuous attention ever since the reports of its presence in the active site of enzymes, such as haloperoxidases and nitrogenases, also including the discovery of its abundance in *Amanita* mushrooms and certain ascidians.[1] In addition, vanadium complexes

[a] Dr. S. Roy, S. Lima, Dr. M. Mohanty, Dr. A. Banerjee, Prof. Dr. R. Dinda
Department of Chemistry, National Institute of Technology
Rourkela 769008, Odisha, India
E-mail: rupamdinda@nitrkl.ac.in

[b] Dr. S. Roy
Department of Sciences, St. Mary's College
Hyderabad 500045, Telangana, India

[c] Dr. M. Böhme, S. Lima, Dr. A. Buchholz, Prof. Dr. W. Plass
Institut für Anorganische und Analytische Chemie
Friedrich-Schiller-Universität Jena
Humboldtstr. 8, 07743 Jena, Germany
E-mail: sekr.plass@uni-jena.de

[d] Dr. S. Rathnam, Dr. I. Banerjee
Department of Biotechnology and Medical Engineering
National Institute of Technology
Rourkela 769008, Odisha, India

[e] Dr. I. Banerjee
Department of Bioscience and Bioengineering
Indian Institute of Technology Jodhpur
Rajasthan 342037, India

[f] Dr. W. Kaminsky
Department of Chemistry, University of Washington Seattle,
Washington 98195, USA

and higher nuclear clusters including polyoxovanadates are also of interest for their attractive chemical, physical, and biological properties pertaining to catalysis, sensor technology, bioinorganic chemistry, and magnetochemistry.[2] In particular, the magnetochemical properties of vanadium complexes are of topical interest and are discussed for potential use as spin qubits.[3] In this context, trinuclear metal complexes with triangular arrangement of ions with non-integer spins are of specific interest, as they can provide access to systems that exhibit spin-electric coupling.[4] However, trinuclear vanadium(IV) compounds with such a spin topology are still rather scarcely reported.[5] From a medicinal point of view,[6] besides the well-established insulin like activity of vanadium compounds,[7] their potential chemotherapeutic application as antitumor drugs inspires the exploration into new vanadium-based anticancer agents,[8,9–12] with a particular interest in those that exhibit specific cytotoxicity towards cancer cells.[13]

Furthermore, the chemistry of transition metal complexes with ligands containing the azo ($-N=N-$) chromophore has attracted attention for their diverse roles in biology, as catalysts, and in the dyes and pigment industry.[14] This can be attributed to specific characteristics related to the azo group such as its π-acidity, interesting coordination modes, and molecular structures as well as redox and photo-physical properties. Our interest in the synthesis of thiazole ring containing azo ligands stems from the observation of a potent antitumor activity by compounds utilizing this heterocyclic moiety.[15] In addition, β-naphthol moieties, are yet another important pharmacophoric core of several anticancer, hypotensive, and bradycardic drugs.[16] Hence, the combined effects of thiazole and β-

Eur. J. Inorg. Chem. **2022**, e202200109 (1 of 8)

© 2022 The Authors. European Journal of Inorganic Chemistry published by Wiley-VCH GmbH

EurJIC
European Journal of Inorganic Chemistry

Research Article
doi.org/10.1002/ejic.202200109

**Chemistry Europe**
European Chemical
Societies Publishing

naphthol have been utilized in the present study to design new azo-based vanadium complexes.

In the present study, we used two thiazolyl based mono-anionic tridentate azo-based ligands that lead to the formation of trinuclear vanadium(IV) complexes. To the best of our knowledge, the synthesized complexes are the first structurally characterized examples possessing a solvent derived μ_3-methoxido bridge with the general formula $[V^{IV}_3O_3(\mu_3\text{-}OMe)(\mu_2\text{-}OMe)_3(L^{1,2})_2]$. The resulting magnetic properties for this trinuclear vanadium(IV) topology were examined by experimental and theoretical methods (DFT and ab initio CASSCF/CASPT2). In addition, for the newly synthesized trinuclear vanadium(IV) complexes with azo-based ligands, the in vitro antiproliferative activity against human cervical (HeLa) and human colon (HT-29) cancer cell lines was examined.

Results and Discussion

Synthesis and Characterization

Two new azo ligands 1-(2-(thiazol-2-yl)diazenyl)naphthalene-2-ol (HL^1) and 2-(2-(thiazol-2-yl)diazenyl)-4-methylphenol (HL^2) were prepared in 60–72 % yield by the coupling of diazotized 2-aminothiazole with β-naphthol (HL^1) and p-cresol (HL^2). The reaction of the azo ligands with vanadyl sulfate in equimolar ratio in the presence of triethylamine under refluxing conditions in methanol solution afforded the trinuclear vanadium(IV) complexes $[V^{IV}_3O_3(\mu_3\text{-}OMe)(\mu_2\text{-}OMe)_3(L^{1,2})_2]$ (**1** and **2**) as depicted in Scheme 1. After cooling, both complexes were isolated directly from the reaction mixture as green crystalline material. The structural formula of the complexes is based on elemental analyses, spectroscopic data, and single crystal X-ray diffraction analysis of complex **1**. The complexes are soluble in acetonitrile but less soluble in water, methanol, and ethanol.
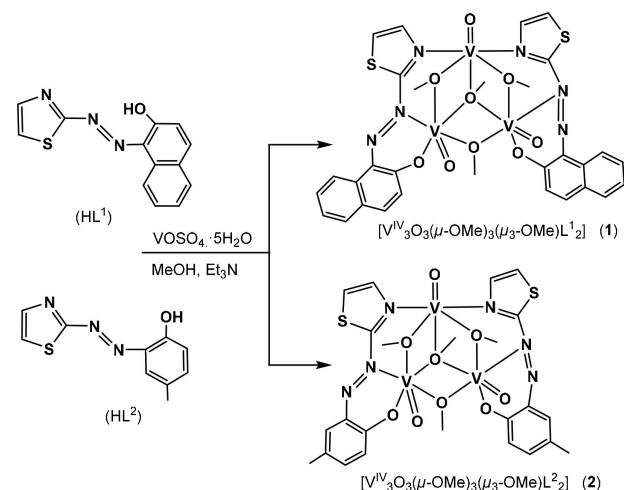
IR stretching frequencies observed in the range of 1504–1532 cm^{-1} in the free ligands HL^{1,2} are attributed to the presence of the azo functional group (—N≡N—), which shift to a lower frequency range of 1494–1485 cm^{-1} upon complexation (**1** and **2**). The presence of strong peaks in the IR spectra of **1** and **2** at 980 and 972 cm^{-1}, respectively, are consistent with a typical V≡O stretching frequency.[17] DFT calculations of vibrational modes for **1** and **2** confirm the observed assignment for the V≡O stretching vibrations (see Table S1 of the Supporting Information). Additional calculated IR frequencies which can be attributed to the $[V^{IV}_3O_3(\mu_3\text{-}OMe)(\mu_2\text{-}OMe)_3]^{2+}$ core in **1** and **2** are also given in Table S1 of the Supporting Information. ESI-MS of complexes **1** and **2** were recorded in acetonitrile solution. A representative ESI-MS spectrum of complex **1** is shown in Figure S1 of the Supporting Information. Mass spectral analysis for **1** and **2** shows predominant peaks at m/z 832.87 and 760.93, respectively. These results are consistent with the presence of the proposed μ-methoxido bridged trivanadium(IV) azo species.

To address the stability of the trinuclear complexes in buffer solutions time-dependent UV/vis spectra have been recorded over a period of 48 h in Tris–HCl buffer (pH 7.4) and Dulbecco's phosphate buffer saline (DPBS) solution. As a representative example, the time-dependent spectra for solutions of complex **1** are depicted in Figure S2 of the Supporting Information. In addition to rather strong bands in the range from 320 to 600 nm that can be attributed to intra ligand and charge-transfer transitions, a weak d-d transition at around 805 to 815 nm is observed.[12] The observed spectra show a slight change over time which is considerably less for the DPBS buffer. These spectral changes might be attributed to partial exchange of ligands at the trinuclear core or dissociation of the complex. However, in the ESI-MS data recorded in acetonitrile solution no evidence for such a behavior could be observed.

X-ray Crystallography

The X-ray crystal structure analysis reveals that complex **1** crystallizes in the monoclinic space group $P2_1/c$ and confirms the trinuclear molecular structure. The crystal data and refinement details are summarized in Table S2 of the Supporting Information. The molecular structure of $[V^{IV}_3O_3(\mu_3\text{-}OMe)(\mu_2\text{-}OMe)_3(L^1)_2]$ (**1**) is depicted in Figure 1 and selected bond lengths and angles are listed in Table S3 of the Supporting Information.

All three vanadium(IV) centers contain an oxido donor with a V≡O bond length of about 1.60 Å. The octahedral coordination sphere of the three ions are completed by two tridentate ligands L^1 providing an NNO donor set and four bridging methoxido groups, one as μ_3-OMe and three as μ_2-OMe. The octahedral coordination environment for all three vanadium centers in **1** is confirmed by continuous shape measures, which give the best fit (smallest S value) for an octahedron and are consistent with the two types of vanadium(IV) centers (V1: $S(O_h) = 1.254$; V2: $S(O_h) = 0.933$; V3: $S(O_h) = 0.909$; for all values see Table S4 of the Supporting Information).[18]

The overall structure can be described as an arrangement of three edge-shared octahedra with one common μ_3-bridging
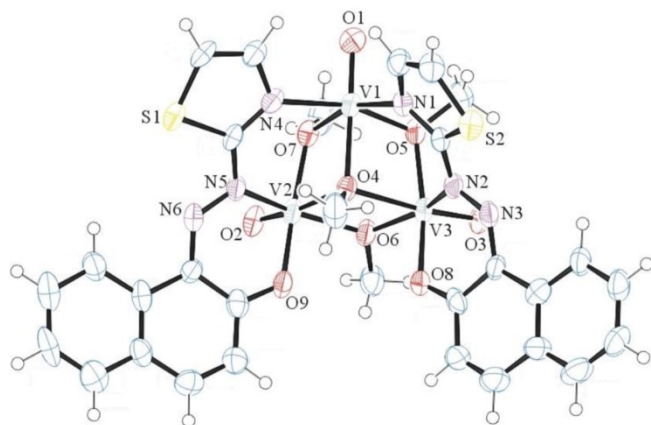

Scheme 1. Schematic diagram for the synthesis of $[V^{IV}_3O_3(\mu_3\text{-}OMe)(\mu_2\text{-}OMe)_3(L^{1,2})_2]$ (**1** and **2**).

EurJIC
European Journal of Inorganic Chemistry

Research Article
doi.org/10.1002/ejic.202200109

Chemistry Europe
European Chemical Societies Publishing

Figure 1. Representation of the molecular structure of of $[V^{IV}_3O_3(\mu_3\text{-OMe})(\mu_2\text{-OMe})_3(L^1)_2]$ (**1**) with displacement parameters at the 50% probability level.

methoxido group. Together with the other three μ_2-bridging methoxido donors this leads to a lacunary heterocubane $\{(VO)_3(\mu_3\text{-OMe})(\mu_2\text{-OMe})_3\}^{2+}$ core unit. To the best of our knowledge, such a trinuclear arrangement of oxidovanadium(IV) groups is unprecedented in literature and leads to an all syn-coplanar configuration of the V=O groups in the edge-shared dinuclear fragments. The two remaining coordination sites at each vanadium(IV) center are occupied differently, resulting in two types of centers: (i) V1 is additionally coordinated by the thiazole nitrogen donors (N1 and N4) of both supporting ligands, while (ii) V2 and V3 are coordinated by the NO chelate of the two ligands L^1, given by the azo nitrogen and the phenolate oxygen donor (V2: N5 and O9; V3: N2 and O8).

This leads to a clear difference in the V—O bond length of the μ_3-bridging methoxido donor O4 with the three vanadium centers, which is significantly smaller for V1 (V1–O4 2.125, V2–O4 2.192, V3–O4 2.208 Å). On the other hand, all six V—O bonds of the μ_2-bridging methoxido groups are rather similar ranging from 1.96 to 2.00 Å and compare well with those observed earlier.[19] The V—O—V bridging angles at the μ_3-OMe and the μ_2-OMe groups again fall into two groups, with the ones that include V1 being somewhat smaller, at about 95 and 107°, respectively. The values observed for the bridging angles V2–O4–V3 (μ_3) and V2–O6–V2 (μ_2) are 97.3 and 111.6°, respectively.

Moreover, the observed variations in the bridging mode and the coordination environment of the vanadium(IV) centers leads to a significant difference in the distances between the vanadium centers with two at about 3.19 Å (V1···V2 and V1···V3) and one somewhat larger at 3.30 Å (V2···V3).

It is also worth noting that the bridging methoxido groups generally show an out-of-plane distortion of the methyl substituent (see Table S5 of the Supporting Information). For the μ_3-OMe group, this distortion is consistent with the observed presence of two types of vanadium centers based on the difference in coordination by the two ligands, leading to angles of about 34° for the bridging planes including the vanadium center V1 and 48° for the plane defined by the

vanadium centers V2 and V3. The situation is different for the three μ_2-OMe groups, for which the steric repulsion with neighboring molecules leads to a significant variation of the corresponding out-of-plane angle in the series of the planes defined by V1/V3, V2/V3, and V1/V2 with values of 27, 31, and 38°, respectively.

Magnetic Properties

The magnetic susceptibility data were measured in the temperature range from 2 to 300 K and the corresponding data depicted in Figure 2. The room temperature χT value is about 0.88 $cm^3\,K\,mol^{-1}$ and is significantly decreasing upon lowering the temperature, indicating a rather strong antiferromagnetic exchange contribution. This value is considerably lower than the spin-only value expected for three independent $S=1/2$ spin centers (1.125 $cm^3\,K\,mol^{-1}$ for $g=2$). With decreasing temperature, the χT value decreases and reaches a low-temperature value of 0.34 $cm^3\,K\,mol^{-1}$ at 2 K which is consistent with an $S=1/2$ ground state. This again is a clear indication for an antiferromagnetic exchange coupling between the vanadium(IV) centers in the complex.

The susceptibility data has been simulated using the spin Hamiltonian $\hat{H} = -J_{12}\hat{S}_1\hat{S}_2 - J_{23}\hat{S}_2\hat{S}_3 - J_{13}\hat{S}_1\hat{S}_3$ for a triangular spin topology for the vanadium(IV) complex (see Figure S3 of the Supporting Information). The best fit of the experimental data was obtained with the parameters $g_{av} = 1.965$ and $J_{av} = J_{12} = J_{13} = J_{23} = -75.5\ cm^{-1}$. This is consistent with the g factors typically observed for vanadium(IV) complexes, which are generally somewhat smaller than the free electron values of two.

The observed antiferromagnetic exchange coupling is consistent with the syn-coplanar arrangement of the oxido groups within the bis-methoxido bridged dinuclear fragments $[VO(\mu\text{-OMe})_2VO]^{2+}$,[20] but at the lower end of the usually observed range.[19,21] Nevertheless, from a theoretical study on the magnetostructural correlation for the $[VO(\mu\text{-OMe})_2VO]^{2+}$
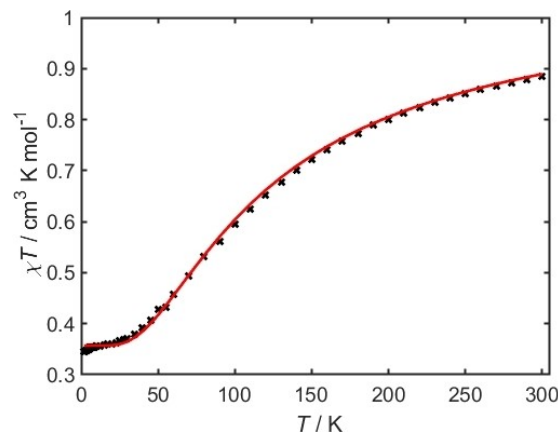

Figure 2. Representation of the temperature dependence χT for **1** at 1000 Oe. The red line represents the best fit with $g_{av} = 1.965$ and $J_{av} = -75.5\ cm^{-1}$ (see text for details).

EurJIC
European Journal of Inorganic Chemistry

Research Article
doi.org/10.1002/ejic.202200109

Chemistry Europe
European Chemical Societies Publishing

core it is clear that on the basis of the given structural parameters (see Table S5 of the Supporting Information) a significant variation should be present for the three individual exchange coupling constants (i.e., $J_{12} \neq J_{13} \neq J_{23}$).[22]

However, an earlier report on trinuclear copper(II) complexes demonstrated that for systems with significantly different coupling constants, these cannot be determined from temperature-dependent magnetic susceptibility data by a common least-square fitting procedure, since the three exchange parameters are strongly correlated for such cases.[23] This is consistent with the fact that independent of the starting values any attempt with three different J values as starting parameters resulted in the above given average values.

Nevertheless, although there is no quantitative relationship, the observed differences for the V–O–V bridging angle of the relevant methoxido groups (O5, O6, and O7) of about 4–5° could easily lead to a variation of about 30 cm^{-1} for the corresponding J values. An additional influence on the J values can be expected from the out-of-plane distortion of the methyl substituent of the relevant bridging methoxido groups (see Table S5 of the Supporting Information). The latter differences in the range between 27 and 38° can attribute for an additional variation of 20–30 cm^{-1} in the values of the individual exchange coupling constants.[22]

To further elucidate the magnetic properties of complex **1** and to probe the expected variation within the three exchange coupling constants, we performed broken-symmetry DFT (BS-DFT) studies. For the calculation of the exchange coupling constants according to the coupling scheme depicted in Figure S3 of the Supporting Information, model structures only allowing for pairwise interactions were utilized, for which the vanadium(IV) centers were subsequently replaced by a diamagnetic titanium(IV) ion (for details see Experimental Section). In a recent work on dinuclear vanadium(IV) compounds, we have demonstrated that a good agreement to the experimental values can be obtained with the density functionals B3LYP and TPSSh.[12] The calculated values for the three different coupling constants between the three individual vanadium(IV) centers (V1, V2, and V3) are summarized in Table S6 of the Supporting Information.

All three J values are antiferromagnetic and show significant differences in the order $|J_{12}| < |J_{23}| < |J_{13}|$. Although the obtained average J values somewhat underestimate the experimental exchange coupling, they are for both functionals virtually identical (B3LYP: -58.6 cm^{-1}; TPSSh: -58.5 cm^{-1}) and still in good agreement with the experimental data ($J_{av} = -75.5$ cm^{-1}). The corresponding spin-density plots can be found in Figure S4 and Figure S5 of the Supporting Information. It should be noted that the magnetic exchange is solely mediated by the μ_2-methoxido ligands (O5, O6, and O7), since in all cases no significant spin density can be observed on the central μ_3-methoxido ligand. This is consistent with the arrangement of the magnetic orbitals within a *syn*-coplanar configuration of the oxido groups for all three dinuclear $[VO(\mu_2\text{-OMe})_2VO]^{2+}$ moieties.[20]

Ab initio multi-reference calculations based on CASSCF/CASPT2/RASSI-SO were performed to determine the magnetic axes and the related g values (for details see Experimental Section). The corresponding energies for the individual vanadium(IV) centers are listed in Table S7 and Table S8 of the Supporting Information. The calculated Cartesian g values are given in Table S9 of the Supporting Information. The average g values obtained for the three vanadium(IV) centers (V1: 1.964; V2: 1.965; V3: 1.964) perfectly agree to the experimentally determined isotropic g value of 1.965. All three vanadium(IV) centers show a weak easy-plane type of anisotropy ($g_{x,y} > g_z$), where the g_z axis is mainly determined by the oxidovanadium bond vector (angle between both vectors: 10.2°/5.0°/5.7° (**V1/V2/V3**); see Figure S6 of the Supporting Information). The somewhat larger angle of intersection observed in case of **V1** (10.2°) might be attributed to the higher distortion of this center from an ideal octahedral coordination sphere (see Table S4 of the Supporting Information).

Cytotoxicity Studies

In the present study, the cytotoxicity of the new trinuclear oxidovanadium(IV) azo complexes **1** and **2** towards the two cancerous cell lines HeLa and HT-29 was investigated.

The studies showed that the trinuclear complexes **1** and **2** can act as potent cytotoxic agents. Plots for the relative cell viability of complexes **1** and **2** against the two cancerous cell lines HeLa and HT-29 are depicted in Figure 3. A comparison of the cell viability at different concentrations of complexes **1** and **2** revealed that the cytotoxic properties of both compounds are rather similar. In the case of HeLa, the IC$_{50}$ values of complex **1** and **2** are 41.4 ± 4.6 and 85.9 ± 7.5 μM, respectively, whereas their IC$_{50}$ values are 5.2 ± 0.5 and 4.6 ± 0.6 μM, respectively, for
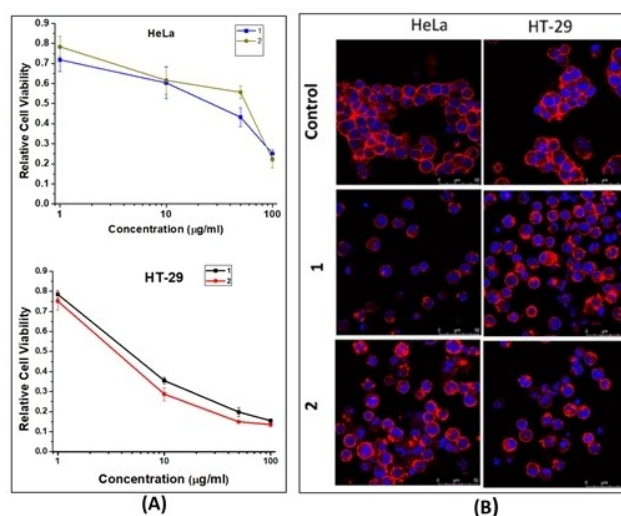

Figure 3. (A) Relative cell viability of **1** and **2** against HeLa and HT-29 cells after 48 h exposure. The data was expressed as mean $\pm$ SD (for $n = 4$). (B) Study of the nucleus fragmentation and cytoskeletal organization of HeLa and HT-29 cells after an exposure to **1** and **2** for 48 h. The experiments were performed in quadruplets. Cells were stained with DAPI (blue color – nucleus) as well as TRITC–Phalloidin (red color – F-actin) and visualized under a confocal microscope.

EurJIC
European Journal of Inorganic Chemistry

Research Article
doi.org/10.1002/ejic.202200109

Chemistry Europe
European Chemical
Societies Publishing

HT-29 cells. The data for both trinuclear vanadium complexes, **1** and **2**, show a significantly higher antiproliferative activity compared to their ligands or metal precursor (IC$_{50}$ > 200 μM). This shows that even the possible presence of small amounts of free ligand or metal ions in the cell culture media cannot lead to a significant effect.

The comparison of the cell viability of complexes **1** and **2** at different concentrations revealed that the cytotoxic properties of both compounds are quite similar against both cell lines tested. In addition, the observed cytotoxicity properties of complexes **1** and **2** are also comparable with commercially available drugs (Table S10 of the Supporting Information).[9,24] It is interesting to note that a comparison of the IC$_{50}$ values of the new trinuclear complexes **1** and **2** with those of the earlier reported dinuclear complexes,[12] which are also based on azo ligands, reveals that the trinuclear complexes are significantly more potent than the dinuclear once in the case of the HT-29 cell line, whereas a reverse trend is observed in the case of HeLa.

As a reference and to address a potential selectivity of the trinuclear complexes **1** and **2**, we also performed a cytotoxicity study against the normal cell line NIH–3T3 (see Figure S7 of the Supporting Information). The IC$_{50}$ values of **1** and **2** against NIH–3T3 are higher than 120 and 130 μM, respectively. This shows a considerably lower toxicity compared to the cancerous cell lines and therefore implies some sort of selectivity.

An analysis of the cytoskeletal organization and structure of the cell nuclei was performed by confocal microscopy for stained cells (see Figure 3). This revealed that under the exposure of complex **1** and **2**, both types of cancerous cells failed to retain their colony and remained as individual cell. A noticeable number of cells were found having a fragmented nucleus, which is associated with apoptotic cell death (Figure 3). Based on such observation, it may be inferred that the cytotoxicity of complexes **1** and **2** is based on the damage of the cell nucleus. This kind of nuclear fragmentation was not observed in the case of the dinuclear oxidovanadium complexes with azo ligands.[12] A probable reason for such variation could be the involvement of different receptors or the variation in permeability of the complexes through nuclear membranes.[25]

As compared to the other vanadium complexes described in the literature, the cytotoxicity of the trinuclear complexes **1** and **2** against colon cancer cells (HT-29) is among the highest antiproliferative efficacies observed to date. Relevant previously reported vanadium(IV/V) complexes are oxidovanadium(V) complexes [LVO(OiPr)] with salan ligands (IC$_{50}$ > 6.8 μM),[9] a mononuclear oxidovanadium(IV) complex [VO(L)$_2$] with dibenzoylmethane (IC$_{50}$ = 16.1 μM),[10] oxidovanadium(V) complexes [LpVO] with diaminotris(phenolato) ligands (IC$_{50}$ > 0.6 μM),[11] and a vanadium(IV) complex [VOL] with a diethylaminophenyl substituted salen-based Schiff base ligand (IC$_{50}$ > 100 μM).[26]

In general, the biotransformation of drugs must be taken into consideration to rationalize the potency of drugs. It has been evidenced in previous reports that based on the conditions, more than one active species might be responsible for rendering cytotoxicity to metal complexes. Multiple factors,

including ligand exchange, redox properties, and other chemical changes, play a vital role in determining the speciation of complexes in organisms.[27] Similar effects can generally be assumed for the trinuclear azo complexes under study.

Nevertheless, it is noteworthy to mention that an increase in cytotoxicity against HT-29 cells with an increase in nuclearity is evident when going from monovanadium (IC$_{50}$ > 47 μM for [VO(sal-L-tryp)(acetylethTSC)]·C$_2$H$_5$OH, [VO(sal-L-tryp)(Me–ATSC)], and [VO(sal-L-tryp)(N-ethymethohcarbthio)]·H$_2$O)[28] to divanadium (IC$_{50}$ > 25.9 μM)[12] and trivanadium complexes, the latter being analyzed in the present study (8.76 and 7.35 μM). However, to substantiate such a possible trend between nuclearity and cytotoxicity further investigations are required. In addition, these biological observations stress the importance of fine-tuning the ligand environment around the vanadium center in order to achieve higher antiproliferative activity.

Conclusion

The synthetic approach to a new type of trinuclear methoxido bridged vanadium(IV) complexes with a lacunary heterocubane core structure, [V$^{IV}_3$O$_3$(μ$_3$-OMe)(μ$_2$-OMe)$_3$(L^{1,2})$_2$] (**1** and **2**), employing monoprotic tridentate 2-(thiazol-2-yl)diazenyl ligands is presented. Besides spectroscopic analysis, further support for the formation of the trivanadium species was obtained from single crystal X-ray diffraction study. It revealed that the complex contains three V(IV) ions, linked by one μ$_3$-OMe and three μ$_2$-OMe groups to a lacunary heterocubane {(VO)$_3$(μ$_3$-OMe)(μ$_2$-OMe)$_3$}$^{2+}$ core unit, which leads to *syn*-coplanar arrangements for all three divanadium fragments. This leads to pairwise antiferromagnetic interactions between the three vanadium(IV) centers, which based on DFT calculations show a significant variation due to the relevant oxygen bridging angle and the out-of-plane distortion of the corresponding methyl substituent of the bridging methoxido group. Spin population analyses show that the antiferromagnetic exchange is mediated by the μ$_2$-methoxido co-ligands, consistent with the *syn*-coplanar bridging mode, and almost no spin density can be found on the central μ$_3$-methoxido co-ligand. The cytotoxicity of complexes **1** and **2** was studied against the cancerous cell lines HeLa and HT-29. Both complexes are among the most potent vanadium complexes known against the colon cancer cell line HT-29 with only a small difference induced by the difference in the ligand backbone. Interestingly, the cytotoxicity of the vanadium complexes against HT-29 cells appears to show a trend suggesting a dependence on their nuclearity, with the highest antiproliferative activity observed for the trinuclear complexes. The results encourage further investigations into mechanistic aspects of the cytotoxicity of this family of complexes, and tests on other cancer cell lines are the scope of future research.

EurJIC
European Journal of Inorganic Chemistry

Research Article
doi.org/10.1002/ejic.202200109

Chemistry Europe
European Chemical
Societies Publishing

Experimental Section

General Methods and Materials: Reagent grade solvents were dried and distilled prior to use. All other chemicals were commercially available with reagent grade and used as received. Dulbecco's Modified Eagle Media (DMEM), Dulbecco's phosphate buffer saline (DPBS), trypsin EDTA solution, Fetal Bovine Serum (FBS), antibiotic-antimitotic solution, and MTT assay kit were purchased from Himedia, Mumbai, India. TRITC–Phalloidin and 4′,6-Diamidin-2-phenylindol (DAPI) were procured from Sigma-Aldrich, India. HeLa, HT-29, and NIH–3T3 cell lines were procured from NCCS, Pune, India. Elemental analyses were performed on a vario ELcube CHNS Elemental analyzer. IR spectra were recorded on a Perkin-Elmer Spectrum RXI spectrometer. ^1H NMR spectra were recorded with a Bruker Ultrashield 400 MHz spectrometer. UV/vis spectra were recorded on a Lamda 25, PerkinElmer spectrophotometer. Mass spectra were obtained on a SQ-300 MS instrument.

Synthesis of Ligands $HL^{1,2}$

The azo ligands $HL^{1,2}$ were prepared in 60–72% yield by the coupling of diazotized 2-aminothiazole (1 g, 10 mmol) with β-naphthol (1.44 g, 10 mmol) (HL^1) and p-cresol (HL^2) (1 mL, 10 mmol) under stirring condition at a temperature below 5 °C. The resulting compounds were washed with water and dried over anhydrous $CaCl_2$. Purified ligands were obtained by slow evaporation of the saturated ethanolic solution of the crude products.

HL^1: Anal. calc. for $C_{13}H_9N_3OS$: C, 61.16; H, 3.55; N, 16.46. Found: C, 61.18; H, 3.58; N, 16.48. IR (KBr pellet, cm^{-1}): $\tilde{\nu} = 3510$ ν(O–H), br; 1504 ν(N=N); 1412 ν(C–O)$_{phenolic}$. ^1H NMR (400 MHz, $CDCl_3$, ppm): $\delta = 14.87$ (s, 1H, OH), 8.55–6.97 (m, 8H, aromatic). ^{13}C NMR (100 MHz, $CDCl_3$, ppm): $\delta = 172.82$–109.50 (13 C atoms, aromatic). Yield: 18.36 mg (71.99 μmol, 72%).

HL^2: Anal. calc. for $C_{10}H_9N_3OS$: C, 54.78; H, 4.14; N, 19.16. Found: C, 54.77; H, 4.16; N, 19.15. IR (KBr pellet, cm^{-1}): $\tilde{\nu} = 3337$ ν(O–H), br; 1532 ν(N=N); 1419 ν(C–O)$_{phenolic}$. ^1H NMR (400 MHz, DMSO-d_6, ppm): $\delta = 10.50$ (s, 1H, OH), 8.05–6.97 (m, 5H, aromatic), 2.23 (s, 3H, –CH$_3$). ^{13}C NMR (100 MHz, DMSO-d_6, ppm): $\delta = 155.06$–118.95 (9 C atoms, aromatic), 20.34 (s, 3H, –CH$_3$). Yield: 13.14 mg (59.99 μmol, 60%).

Synthesis of complexes $[V^{IV}_3O_3(\mu_3\text{-OMe})(\mu_2\text{-OMe})_3(L^{1,2})_2]$ (1 and 2)

$[V^{IV}_3O_3(\mu_3\text{-OMe})(\mu_2\text{-OMe})_3(L^1)_2]$ (1): Triethylamine (1 mmol) was added to a methanolic solution (15 mL) of the ligand HL^1 (1 mmol, 255 mg) under refluxing condition. $VOSO_4 \cdot 5H_2O$ (1 mmol, 253 mg) was then added to the refluxing solution. The color of the solution changed to purple after one hour of reflux. Reflux was continued for 68 h. A dirty green crystalline residue was isolated upon filtration. Yield: 54 mg (64.83 μmol, 65%). Anal. calc. for $C_{30}H_{28}N_6O_9S_2V_3$: C, 43.23; H, 3.39; N, 10.08. Found: C, 43.26; H, 3.46; N, 10.02. IR (KBr pellet, cm^{-1}): $\tilde{\nu} = 1494$ ν(N=N); 980 br ν(V=O). ESI-MS (CH_3CN; negative ion mode): m/z 832.87 $[M]^-$.

$[V^{IV}_3O_3(\mu_3\text{-OMe})(\mu_2\text{-OMe})_3(L^2)_2]$ (2): This complex was obtained as greenish black amorphous product following the same synthetic procedure adopted for **1** using ligand HL^2 (1 mmol, 219 mg). Yield: 46 mg (60.45 μmol, 61%). Anal. calc. for $C_{24}H_{28}N_6O_9S_2V_3$: C, 37.86; H, 3.71; N, 11.04. Found: C, 37.93; H, 3.79; N, 11.09. IR (KBr pellet, cm^{-1}): $\tilde{\nu} = 1485$ ν(N=N); 972 br ν(V=O). ESI-MS (CH_3CN; negative ion mode): m/z 760.93 $[M]^-$.

X-Ray Crystallography: A black prism of **1** measuring 0.040 × 0.020 × 0.020 mm^3 was mounted on a loop with oil. Data was collected at −173 °C on a Bruker APEX II single crystal X-ray diffractometer (Mo-radiation). Crystal-to-detector distance was 40 mm and exposure time was 180 s per frame for all sets. The scan width was 0.5°. Data collection was 100% complete to 25° in ϑ. A total of 38402 full and partial reflections were collected covering the indices, $-21 \leq h \leq 20$, $-27 \leq k \leq 27$, $-10 \leq l \leq 10$. 6100 reflections were symmetry independent and the $R_{int} = 0.1233$ reflects the small sample size. Indexing and unit cell refinement indicated a primitive monoclinic lattice. The space group was found to be $P2_1/c$ (No. 14). The data were integrated and scaled using SAINT, SADABS within the APEX2 software package by Bruker. Solution by direct methods (SHELXS, SIR97)[29] produced a complete heavy atom phasing model consistent with the proposed structure. The structure was completed by difference Fourier synthesis with SHELXL.[30] Scattering factors were taken from Waasmair and Kirfel.[31] Hydrogen atoms were placed in geometrically idealized positions and constrained to ride on their parent atoms with C–H distances in the range 0.95–1.00 Å. Isotropic thermal parameters U_{eq} were fixed such that they were 1.2 U_{eq} of their parent atom U_{eq} for CH and 1.5 U_{eq} of their parent atom U_{eq} in case of methyl groups. All non-hydrogen atoms were refined anisotropically by full-matrix least-squares. Table S2 of the Supporting Information summarizes the data collection details.

Magnetic Measurements: Magnetic susceptibilities data were obtained from powdered samples in gelatine capsules at 1000 Oe using a Quantum-Design MPMS-5 SQUID magnetometer equipped with a 5 Tesla magnet in the range from 2 to 300 K. The data is corrected for the sample holder and the diamagnetic moment of the sample.[32] The data was simulated using the MagProp package of DAVE (Data Analysis and Visualization Environment, www.ncnr.nist.gov/dave). For data calculation and graphics Matlab 2018a was used.

Computational Details: The computational studies for **1** were performed with the Turbomole package of programs (version 7.2).[33] Structural data in terms of atomic positions were taken from the X-ray crystallographic structure of **1** for which the position of the hydrogen atoms were energy optimized prior to single-point calculations. These optimizations were carried out at RI-DFT[34]/BP86[35]/def2-SVP[36] level of theory for the high-spin state (S = 3/2). Subsequently, single-point calculations utilizing dinuclear vanadium model structures with one vanadium center replaced by a diamagnetic titanium(IV) ion were performed for the high-spin (HS) and broken-symmetry (BS) states with the B3LYP[37,38] and TPSSh[39] density functionals (for structural models – **V1V2**, **V1V3**, **V2V3** – see Figure S8 of the Supporting Information). In all calculations the triple-ζ def2-TZVPP basis sets were used together with a tight SCF energy convergence criterion (10^{-8} au). The BS-DFT based magnetic coupling constants were calculated for an isotropic Heisenberg Hamiltonian ($\hat{H} = -J\hat{S}_1\hat{S}_2$) according to Yamaguchi's approach as given in Equation (1).[40]

$$J = \frac{2(E_{BS} - E_{HS})}{\langle S^2_{HS} \rangle - \langle S^2_{BS} \rangle} \tag{1}$$

In order to calculate the vibrational modes of the two presented complexes, the atomic position data of **1** as obtained by X-ray crystallography was optimized with Turbomole at the RI-DFT-D3[37,38,41]/BP86[35]/def2-TZVPP[36] level of theory. The vibrational modes have been calculated on the basis of the DFT-optimized structure at the exact same level of theory. All calculated harmonic IR frequencies were calibrated by a scaling factor of 0.988. Due to a lack of X-ray crystallographic data for **2**, the DFT-optimized molecular structure of **1** was modified at the ligand backbone in order to generate a molecular structure for **2** which was then optimized in order to obtain the corresponding calculated vibrational modes for **2**. *Ab initio* multi-reference computational studies

for **1** were performed with the MOLCAS 8.0 SP1 package of programs.[42] For all calculations ANO-RCC basis sets[43] have been used (basis set details are given in Table S11 of the Supporting Information) in combination with a scalar-relativistic second-order Douglas-Kroll-Hess Hamiltonian. These calculations were based on the three structural models derived from the above mentioned model structure with optimized positions of the hydrogen atoms (see Figure S8 of the Supporting Information) for which suggestively two of the three vanadium(IV) centers have been replaced by diamagnetic titanium(IV) ions (for structural models **V1**–**V3** see Figure S9 of the Supporting Information). State-average CASSCF calculations with one electron in five orbitals (3d shell) for five states (^{2}D term) were performed for all three centers. Subsequently, dynamic correlation was added by performing CASPT2 calculations based on the state-average CASSCF wave function. Finally, the RASSI-SO module was employed to include spin-orbit coupling. The Cartesian g factors and the orientation of the magnetic axes were obtained for all three individual vanadium(IV) centers by the SINGLE_ANISO module.

Cytotoxicity study: Cytotoxic properties of complexes **1** and **2** were evaluated *in vitro* using two human cancer cell lines, namely HeLa (human cervical cancer cell line) and HT-29 (human colon cancer cell line), and the non-cancerous cell line NIH−3T3 (non-cancerous mouse embryonic fibroblast cell line). For this purpose, cells were cultured in DMEM media supplemented with 10% FBS in an incubator (5% CO_2, 95% humidity, and 37°C). During the experiment, cells were harvested by trypsinization, seeded in the well of a 96 well tissue culture plate at a concentration of 1×10^4 cells/well, and kept inside the incubator. After 12 h of cell seeding, complexes **1** and **2** were added to the cells at four different concentrations (HT-29 and HeLa: 1, 10, 50, and 100 µg/mL; NIH−3T3 (5, 10, 50, and 100 µg/mL). For this purpose, both the complexes were initially dissolved in DMSO at a concentration of 4 mg/mL and then diluted in the cell culture media. The cells were treated with the complexes for 48 h. After that, the viability of the cells was assessed by the MTT assay using a commercially available MTT assay kit. The relative viability of the cells after treatment was reported in terms of cell viability index as per Equation (2). All the experiments were performed for three independent batches of cell cultures in quadruplets, and the data were expressed as mean $\pm$ SD. Single variance ANOVA under 95% confidence interval was used to evaluate the statistical significance of the data. From the MTT data, IC_{50} values were determined by interpolation[44] using standard procedures available in the software package Origin.[45]

$$\text{cell viability index} = \frac{\textit{sample absorbance at 595 nm}}{\textit{control absorbance at 595 nm}} \quad (2)$$

The effect of **1** and **2** on the cytoskeletal organization and the integrity of the structure of the cell nuclei of the cancerous cell lines were examined using confocal microscopy (Leica, SP8). For this study, cells were incubated with **1** and **2** for 48 h, as mentioned above. After that, cells were washed gently with PBS, fixed with 4% paraformaldehyde for 15 min and permeabilized (using 0.25% Triton X-100 in PBS, 10 min exposure). Post-permeabilization cells were stained with DAPI (for nucleus staining) and TRITC−phalloidin (for F-actin staining).[46]

Deposition Number 1859448 (for **1**) contains the supplementary crystallographic data for this paper. These data are provided free of charge by the joint Cambridge Crystallographic Data Centre and Fachinformationszentrum Karlsruhe Access Structures service www.ccdc.cam.ac.uk/structures.

Conflict of Interest

The authors declare no conflict of interest.

Data Availability Statement

The data that support the findings of this study are available in the supplementary material of this article.

[1] a) K. Kustin, J. Costa Pessoa, D. C. Crans (Hrsg.) *ACS symposium series*, Vol. 974, American Chemical Society, Washington, DC, **2007**; b) D. Rehder, *Bioinorganic Vanadium Chemistry*, Wiley, Chichester, **2008**; c) D. C. Crans, J. J. Smee, E. Gaidamauskas, L. Yang, *Chem. Rev.* **2004**, *104*, 849–902; d) D. Rehder, *Metallomics* **2015**, *7*, 730–742; e) J. Costa Pessoa, E. Garribba, M. F. Santos, T. Santos-Silva, *Coord. Chem. Rev.* **2015**, *301–302*, 49–86; f) D. Rehder, G. Santonin, G. M. Licini, C. Schulzke, B. Meier, *Coord. Chem. Rev.* **2003**, *237*, 53–63; g) W. Plass, *Coord. Chem. Rev.* **2011**, *255*, 2378–2387; h) P. Zanello, *Coord. Chem. Rev.* **2019**, *398*, 113004; i) R. R. Eady, *Coord. Chem. Rev.* **2003**, *237*, 23–30; j) W. Plass, *J. Mol. Struct.* **1994**, *121*, 53–62; k) W. Plass, *Angew. Chem. Int. Ed.* **1999**, *38*, 909–912; *Angew. Chem.* **1999**, *111*, 960–962.

[2] a) R. R. Langeslay, D. M. Kaphan, C. L. Marshall, P. C. Stair, A. P. Sattelberger, M. Delferro, *Chem. Rev.* **2019**, *119*, 2128–2191; b) M. R. Maurya, *Coord. Chem. Rev.* **2019**, *383*, 43–81; c) Y. Hayashi, *Coord. Chem. Rev.* **2011**, *255*, 2270–2280; d) A. Dolbecq, E. Dumas, C. R. Mayer, P. Mialane, *Chem. Rev.* **2010**, *110*, 6009–6048; e) J. M. Clemente-Juan, E. Coronado, A. Gaita-Ariño, *Chem. Soc. Rev.* **2012**, *41*, 7464–7478; f) D. Rehder, *Inorg. Chim. Acta* **2017**, *455*, 378–389; g) W. Plass, *Coord. Chem. Rev.* **2003**, *237*, 205–212; h) M. Aureliano, N. I. Gumerova, G. Sciortino, E. Garribba, A. Rompel, D. C. Crans, *Coord. Chem. Rev.* **2021**, *447*, 214143; i) M. Aureliano, N. I. Gumerova, G. Sciortino, E. Garribba, C. C. McLauchlan, A. Rompel, D. C. Crans, *Coord. Chem. Rev.* **2022**, *454*, 214344.

[3] a) M. Trif, F. Troiani, D. Stepanenko, D. Loss, *Phys. Rev. B* **2010**, *82*, 45429; b) K.-Y. Choi, Z. Wang, H. Nojiri, J. van Tol, P. Kumar, P. Lemmens, B. S. Bassil, U. Kortz, N. S. Dalal, *Phys. Rev. Lett.* **2012**, *108*, 67206; c) J. M. Zadrozny, J. Niklas, O. G. Poluektov, D. E. Freedman, *ACS Cent. Sci.* **2015**, *1*, 488–492; d) M. Atzori, L. Tesi, E. Morra, M. Chiesa, L. Sorace, R. Sessoli, *J. Am. Chem. Soc.* **2016**, *138*, 2154–2157.

[4] a) A. K. Boudalis, J. Robert, P. Turek, *Chem. Eur. J.* **2018**, *24*, 14896–14900; b) J. Liu, J. Mrozek, W. K. Myers, G. A. Timco, R. E. P. Winpenny, B. Kintzel, W. Plass, A. Ardavan, *Phys. Rev. Lett.* **2019**, *122*, 37202; c) J. Robert, N. Parizel, P. Turek, A. K. Boudalis, *J. Am. Chem. Soc.* **2019**, *141*, 19765–19775; d) B. Kintzel, M. Fittipaldi, M. Böhme, A. Cini, L. Tesi, A. Buchholz, R. Sessoli, W. Plass, *Angew. Chem. Int. Ed.* **2021**, *60*, 8832–8838; *Angew. Chem.* **2021**, *133*, 8914–8920.

[5] a) D. Gatteschi, R. Sessoli, W. Plass, A. Müller, E. Krickemeyer, J. Meyer, D. Sölter, P. Adler, *Inorg. Chem.* **1996**, *35*, 1926–1934; b) T. Yamase, E. Ishikawa, K. Fukaya, H. Nojiri, T. Taniguchi, T. Atake, *Inorg. Chem.* **2004**,

EurJIC
European Journal of Inorganic Chemistry

Research Article
doi.org/10.1002/ejic.202200109

Chemistry
Europe
European Chemical
Societies Publishing

43, 8150–8157; c) H. Theil, C.-G. Freiherr von Richthofen, A. Stammler, H. Bögge, T. Glaser, *Inorg. Chim. Acta* **2008**, *361*, 916–924; d) J. S. Maass, Z. Chen, M. Zeller, F. Tuna, R. E. P. Winpenny, R. L. Luck, *Inorg. Chem.* **2012**, *51*, 2766–2776; e) L. D. Sanjeewa, M. A. McGuire, C. D. McMillen, V. O. Garlea, J. W. Kolis, *Chem. Mater.* **2017**, *29*, 1404–1412.

[6] a) A. Ścibior, Ł. Pietrzyk, Z. Plewa, A. Skiba, *J. Trace Elem. Med. Biol.* **2020**, *61*, 126508; b) J. Costa Pessoa, S. Etcheverry, D. Gambino, *Coord. Chem. Rev.* **2015**, *301*, 24–48.

[7] a) S. Treviño, A. Diaz, *J. Inorg. Biochem.* **2020**, *208*, 111094; b) K. H. Thompson, J. Lichter, C. LeBel, M. C. Scaife, J. H. McNeill, C. Orvig, *J. Inorg. Biochem.* **2009**, *103*, 554–558.

[8] a) E. Kioseoglou, S. Petanidis, C. Gabriel, A. Salifoglou, *Coord. Chem. Rev.* **2015**, *301–302*, 87–105; b) S. Banerjee, A. Dixit, A. A. Karande, A. R. Chakravarty, *Eur. J. Inorg. Chem.* **2015**, 447–457; c) B. Balaji, B. Balakrishnan, S. Perumalla, A. A. Karande, A. R. Chakravarty, *Eur. J. Med. Chem.* **2015**, *92*, 332–341; d) C. Datta, D. Das, P. Mondal, B. Chakraborty, M. Sengupta, C. R. Bhattacharjee, *Eur. J. Med. Chem.* **2015**, *97*, 214–224.

[9] L. Reytman, O. Braitbard, E. Y. Tshuva, *Dalton Trans.* **2012**, *41*, 5241–5247.

[10] M. Mohamadi, S. Yousef Ebrahimipour, M. Torkzadeh-Mahani, S. Foro, A. Akbari, *RSC Adv.* **2015**, *5*, 101063–101075.

[11] L. Reytman, O. Braitbard, J. Hochman, E. Y. Tshuva, *Inorg. Chem.* **2016**, *55*, 610–618.

[12] S. Roy, M. Böhme, S. P. Dash, M. Mohanty, A. Buchholz, W. Plass, S. Majumder, S. Kulanthaivel, I. Banerjee, H. Reuter, W. Kaminsky, R. Dinda, *Inorg. Chem.* **2018**, *57*, 5767–5781.

[13] a) S. Banerjee, A. Dixit, A. A. Karande, A. R. Chakravarty, *Dalton Trans.* **2016**, *45*, 783–796; b) S. Banerjee, A. Dixit, R. N. Shridharan, A. A. Karande, A. R. Chakravarty, *Chem. Commun.* **2014**, *50*, 5590–5592.

[14] a) S. Benkhaya, S. M'rabet, A. El Harfi, *Heliyon* **2020**, *6*, e03271; b) S. Crespi, N. A. Simeth, B. König, *Nat. Chem. Rev.* **2019**, *3*, 133–146; c) H. Mutlu, C. M. Geiselhart, C. Barner-Kowollik, *Mater. Horiz.* **2018**, *5*, 162–183; d) N. M. Aljamali, *Biochem. Anal. Biochem.* **2015**, *4*, 1000169; e) A. Bianchi, E. Delgado-Pinar, E. García-España, C. Giorgi, F. Pina, *Coord. Chem. Rev.* **2014**, *260*, 156–215; f) S. Kawata, Y. Kawata, *Chem. Rev.* **2000**, *100*, 1777–1788.

[15] a) L. J. Lombardo, F. Y. Lee, P. Chen, D. Norris, J. C. Barrish, K. Behnia, S. Castaneda, L. A. M. Cornelius, J. Das, A. M. Doweyko, C. Fairchild, J. T. Hunt, I. Inigo, K. Johnston, A. Kamath, D. Kan, H. Klei, P. Marathe, S. Pang, R. Peterson, S. Pitt, G. L. Schieven, R. J. Schmidt, J. Tokarski, M.-L. Wen, J. Wityak, R. M. Borzilleri, *J. Med. Chem.* **2004**, *47*, 6658–6661; b) H. El-Subbagh, A. Al-Obaid, *Eur. J. Med. Chem.* **1996**, *31*, 1017–1021.

[16] B. Das, C. R. Reddy, J. Kashanna, S. K. Mamidyala, C. G. Kumar, *Med. Chem. Res.* **2012**, *21*, 3321–3325.

[17] a) J. Selbin, *Coord. Chem. Rev.* **1966**, *1*, 293–314; b) W. Plass, *Eur. J. Inorg. Chem.* **1998**, 799–805.

[18] a) M. Pinsky, D. Avnir, *Inorg. Chem.* **1998**, *37*, 5575–5582; b) S. Alvarez, D. Avnir, M. Llunell, M. Pinsky, *New J. Chem.* **2002**, *26*, 996–1009.

[19] W. Plass, *Inorg. Chem.* **1997**, *36*, 2200–2205.

[20] W. Plass, *Angew. Chem. Int. Ed. Engl.* **1996**, *35*, 627–631; *Angew. Chem.* **1996**, *108*, 699–703.

[21] a) M. I. Khan, Y.-D. Chang, Q. Chen, J. Salta, Y.-S. Lee, C. J. O'Connor, J. Zubieta, *Inorg. Chem.* **1994**, *33*, 6340–6350; b) W. Plass, *Z. Anorg. Allg. Chem.* **1997**, *623*, 1290–1298.

[22] A. Rodríguez-Fortea, P. Alemany, S. Alvarez, E. Ruiz, *Eur. J. Inorg. Chem.* **2004**, 143–153.

[23] G. V. Baryshnikov, B. F. Minaev, A. T. Baryshnikova, H. Ågren, *Chem. Phys.* **2017**, *491*, 48–55.

[24] a) K. Takara, T. Sakaeda, T. Yagami, H. Kobayashi, N. Ohmoto, M. Horinouchi, K. Nishiguchi, K. Okumura, *Biol. Pharm. Bull.* **2002**, *25*, 771–778; b) L. Petinari, L. K. Kohn, J. E. de Carvalho, S. C. Genari, *Cell Biol. Int.* **2004**, *28*, 531–539; c) A. D. Lewis, L. M. Forrester, J. D. Hayes, C. J. Wareing, J. Carmichael, A. L. Harris, M. Mooghen, C. R. Wolf, *Br. J. Cancer* **1989**, *60*, 327–331; d) A. Stockert, D. Kinder, M. Christ, K. Amend, A. Aulthouse, *Aust. J. Pharm. Ther.* **2014**, *2*, 6.

[25] R. Zhang, X. Qin, F. Kong, P. Chen, G. Pan, *Drug Delivery* **2019**, *26*, 328–342.

[26] M. Rocha, M. C. Ruiz, G. A. Echeverría, O. E. Piro, A. L. Di Virgilio, I. E. León, A. Frontera, D. M. Gil, *New J. Chem.* **2019**, *43*, 18832–18842.

[27] a) A. Levina, D. C. Crans, P. A. Lay, *Coord. Chem. Rev.* **2017**, *352*, 473–498; b) J. Costa Pessoa, I. Correia, *Inorganics* **2021**, *9*, 17; c) P. Nunes, I. Correia, I. Cavaco, F. Marques, T. Pinheiro, F. Avecilla, J. Costa Pessoa, *J. Inorg. Biochem.* **2021**, *217*, 111350; d) E. Griffin, A. Levina, P. A. Lay, *J.*

Inorg. Biochem. **2019**, *201*, 110815; e) A. Banerjee, S. P. Dash, M. Mohanty, G. Sahu, G. Sciortino, E. Garribba, M. F. N. N. Carvalho, F. Marques, J. Costa Pessoa, W. Kaminsky, K. Brzezinski, R. Dinda, *Inorg. Chem.* **2020**, *59*, 14042–14057; f) Y. Yoshikawa, H. Sakurai, D. C. Crans, G. Micera, E. Garribba, *Dalton Trans.* **2014**, *43*, 6965–6972; g) M. Le, O. Rathje, A. Levina, P. A. Lay, *J. Biol. Inorg. Chem.* **2017**, *22*, 663–672; h) D. Sanna, V. Ugone, G. Micera, P. Buglyó, L. Bíró, E. Garribba, *Dalton Trans.* **2017**, *46*, 8950–8967; i) D. Sanna, J. Palomba, G. Lubinu, P. Buglyó, S. Nagy, F. Perdih, E. Garribba, *J. Med. Chem.* **2019**, *62*, 654–664; j) G. Sahu, A. Banerjee, R. Samanta, M. Mohanty, S. Lima, E. R. T. Tiekink, R. Dinda, *Inorg. Chem.* **2021**, *60*, 15291–15309; k) S. A. Patra, M. Mohanty, A. Banerjee, S. Kesarwani, F. Henkel, H. Reuter, R. Dinda, *J. Inorg. Biochem.* **2021**, *224*, 111582.

[28] N. A. Lewis, F. Liu, L. Seymour, A. Magnusen, T. R. Erves, J. F. Arca, F. A. Beckford, R. Venkatraman, A. González-Sarrías, F. R. Fronczek, D. G. Vanderveer, N. P. Seeram, A. Liu, W. L. Jarrett, A. A. Holder, *Eur. J. Inorg. Chem.* **2012**, 664–677.

[29] a) A. Altomare, G. Cascarano, C. Giacovazzo, A. Guagliardi, *J. Appl. Crystallogr.* **1993**, *26*, 343–350; b) A. Altomare, M. C. Burla, M. Camalli, G. L. Cascarano, C. Giacovazzo, A. Guagliardi, A. G. G. Moliterni, G. Polidori, R. Spagna, *J. Appl. Crystallogr.* **1999**, *32*, 115–119.

[30] a) S. Mackay, C. Edwards, A. Henderson, C. Gilmore, N. Stewart, K. Shankland, A. Donald, *MaXus: a computer program for the solution and refinement of crystal structures from diffraction data*, University of Glasgow, Scotland, **1997**; b) G. M. Sheldrick, *SHELXL-97*. Program for the Refinement of Crystal Structures, University of Göttingen, Göttingen, Germany, **1997**; c) G. M. Sheldrick, *Acta Crystallogr.* **2015**, *C71*, 3–8.

[31] D. Waasmaier, A. Kirfel, *Acta Crystallogr.* **1995**, *A51*, 416–431.

[32] E. T. Spielberg, A. Gilb, D. Plaul, D. Geibig, D. Hornig, D. Schuch, A. Buchholz, A. Ardavan, W. Plass, *Inorg. Chem.* **2015**, *54*, 3432–3438.

[33] *TURBOMOLE V7.2.* Development of University of Karlsruhe and Forschungszentrum Karlsruhe GmbH, 1989–2007, TURBOMOLE GmbH, available from http://www.turbomole.com, **2017**.

[34] a) J. L. Whitten, *J. Chem. Phys.* **1973**, *58*, 4496–4501; b) C. van Alsenoy, *J. Comput. Chem.* **1988**, *9*, 620–626; c) B. I. Dunlap, J. W. D. Connolly, J. R. Sabin, *J. Chem. Phys.* **1979**, *71*, 3396–3402; d) E. J. Baerends, D. E. Ellis, P. Ros, *Chem. Phys.* **1973**, *2*, 41–51.

[35] J. P. Perdew, *Phys. Rev. B* **1986**, *33*, 8822–8824.

[36] F. Weigend, R. Ahlrichs, *Phys. Chem. Chem. Phys.* **2005**, *7*, 3297–3305.

[37] C. Lee, W. Yang, R. G. Parr, *Phys. Rev. B* **1988**, *37*, 785–789.

[38] A. D. Becke, *J. Chem. Phys.* **1993**, *98*, 5648–5652.

[39] J. Tao, J. P. Perdew, V. N. Staroverov, G. E. Scuseria, *Phys. Rev. Lett.* **2003**, *91*, 146401.

[40] a) K. Yamaguchi, T. Tsunekawa, Y. Toyoda, T. Fueno, *Chem. Phys. Lett.* **1988**, *143*, 371–376; b) T. Soda, Y. Kitagawa, T. Onishi, Y. Takano, Y. Shigeta, H. Nagao, Y. Yoshioka, K. Yamaguchi, *Chem. Phys. Lett.* **2000**, *319*, 223–230.

[41] S. Grimme, J. Antony, S. Ehrlich, H. Krieg, *J. Chem. Phys.* **2010**, *132*, 154104.

[42] a) F. Aquilante, J. Autschbach, R. K. Carlson, L. F. Chibotaru, M. G. Delcey, L. de Vico, I. Fdez Galván, N. Ferré, L. M. Frutos, L. Gagliardi, M. Garavelli, A. Giussani, C. E. Hoyer, G. Li Manni, H. Lischka, D. Ma, P. Å. Malmqvist, T. Müller, A. Nenov, M. Olivucci, T. B. Pedersen, D. Peng, F. Plasser, B. Pritchard, M. Reiher, I. Rivalta, I. Schapiro, J. Segarra-Martí, M. Stenrup, D. G. Truhlar et al., *J. Comput. Chem.* **2016**, *37*, 506–541; b) F. Aquilante, L. de Vico, N. Ferré, G. Ghigo, P.-A. Malmqvist, P. Neogrády, T. B. Pedersen, M. Pitonák, M. Reiher, B. O. Roos, L. Serrano-Andrés, M. Urban, V. Veryazov, R. Lindh, *J. Comput. Chem.* **2010**, *31*, 224–247.

[43] B. O. Roos, V. Veryazov, P.-O. Widmark, *Theor. Chem. Acc.* **2004**, *111*, 345–351.

[44] L. Serpe, M. Catalano, R. Cavalli, E. Ugazio, O. Bosco, R. Canaparo, E. Muntoni, R. Frairia, M. Gasco, M. Eandi, *Eur. J. Pharm. Biopharm.* **2004**, *58*, 673–680.

[45] *Origin*, Version 2021. OriginLab Corporation, Northampton, MA, USA.

[46] X. Wang, M. Tanaka, S. Krstin, H. S. Peixoto, C. C. de Melo Moura, M. Wink, *Eur. J. Pharmacol.* **2016**, *789*, 265–274.